16th World Conference on Earthquake, 16WCEE 2017
Santiago Chile, January 9th to 13th 2017
Paper N° 1159 (Abstract ID)
Registration Code: S-G1464702234

Variation of Response Spectra and Group Delay Time of Ground Motions in the Kanto Basin, Japan

Y. TERASHIMA [1], Y. SATO [2]

[1] *Researcher, R&D Institute, Takenaka Corporation, Chiba, Japan,terashima.yoshihiro@takenaka.co.jp*
[2] *Group Reader, R&D Institute, Takenaka Corporation, Chiba, Japan,sato.yoshiyukia@takenaka.co.jp*

Abstract

To avoid resonance of long-period structures, an estimation of the variation of long-period ground motion is important. However, variation of the characteristics of ground motion with an azimuth angle has not been sufficiently researched based on observation records of strong motion. In this paper, we focused on the variation of the characteristics of long-period ground motion observed in the Kanto Basin, Japan, due to the path and subsurface of the sedimentary basin. We evaluated the response spectrum and group delay time of the records using indices of ground motion characteristics.

The response spectrum and the group delay time were calculated for several earthquake groups that were divided based on hypocenter locations and azimuth angle from the station. The relation between the groups, the variation of response spectrum, and group delay time were quantitatively analyzed and discussed.

Consequently, it was found that the response spectrum and group delay time of the ground motion have different characteristics in each grouped area. In particular, the shapes of the response spectra for the long-period ranging from 2 s to 10 s varied depending on the area`s direction.

Keywords: Long-Period Ground Motion, Variation of Ground Motion, the Kanto Basin, Japan

1. Introduction

In sedimentary basins such as the Kanto Basin in Japan, the long-period ground motion, which is defined as the period of 2 s-10 s for this paper, has developed strongly. This ground motion may be the cause of resonance of long-period structures.

According to previous studies, the characteristics of long-period ground motion vary with the azimuth angle of the seismic wave due to the difference of the path from the source to the edge of the basin and the path in the sedimentary basin. For example, Hirai and Fukuwa [1] and Terashima et al. [2] found that the earthquake predominant periods at basin sites varied with the direction of the seismic propagation based on numerical simulations using 3D basin models. Zama [3], Uetake [4] and Tsuno et al. [5] also pointed out the variations based on earthquake records observed around the Kanto Basin. In addition, Furumura [6] inferred that the variation in the surface wave excitation is related to the path difference in the basin structure based on large earthquake records.

To reflect the variation of the long-period ground motions to ground motion predictions, the dependence of the variation on the locations of the hypocenters needs to be confirmed. To confirm the dependence, in this study, the hypocenters of the analyzed records were divided into some groups, and then the relationship between the characteristics of long-period ground motion and the regions of the hypocenters, particularly the dependence of the variation of long-period ground motions on the regions, was analyzed. The variations were evaluated based on an about 110 records that also included medium-sized earthquake records. In addition to amplitude characteristics, which were a primary focus in previous studies, phase characteristics were also investigated, as they can be important factors in time series predictions.

2. Analysis of Earthquakes Ground Motion Records in the Kanto Area of Japan

Earthquake records obtained by the Strong-motion Seismograph Networks (K-NET, KiK-net) [7] were used. Figure 1 shows the location of the earthquakes and the recording stations selected. Earthquakes with a magnitude of 5.0 or over, as observed at TKY007 (Shinjuku) from 1996 to 2015, were selected. Table 1 shows the outline of the recording stations. Three stations in the Kanto Basin were selected and referenced as the "basin sites" here after. Three stations around the edge of the basin were also selected and here referenced as the "rock sites". At the rock sites, the velocity of the S wave (V_S) reached 2.5 km/s at depths shallower than 100 m. Each record was selected on the basis of hypocenter depth shallower than 100 km and hypocentral distance closer than 500 km. The signal to noise ratio was confirmed to be at a sufficient level based on the long-period. The locations of the earthquakes were divided into groups to analyze the relationships between the groups and the characteristics of the records.

The earthquake groups were referenced as groups *a* - *k*. An outline of each group is given in Table 2. Group *a* consisted of inland earthquakes including the main shock and aftershocks of the Niigata-ken Chuetsu earthquake (Mw 6.6) that occurred on 23 October 2004. Group *b* was located almost directly under the Kanto Basin. Earthquakes that occurred on the Pacific Ocean side were scattered and were divided into groups *c*, *d*, *f*, and *k*. Groups *c*, *d*, *f*, and *k* consisted of inter-plate earthquakes or intraplate earthquakes at the subduction zone of the Pacific Ocean Plate. Group *e* consisted of inland earthquakes and was shallower than the neighboring group *d*. Groups *g*, *h*, *i*, and *j* were located south of the Kanto Basin. Group *g* consisted of shallow earthquakes east of the Izu Peninsula. Group *h* consisted of intraplate earthquakes around the Nankai Trough southeast of the Kii Peninsula earthquake (Mw 7.4) that occurred on 5 September 2004, including the main shock and aftershocks. Group *i* consisted of intraplate earthquakes around the Suruga Trough. Earthquakes in group *j* occurred near the triple junction where the Philippine Sea Plate, Pacific Ocean Plate, and North American Plate are subducting or colliding.

The pseudo velocity response spectra ${}_pS_V$ were computed as the amplitude characteristics of ground motions. In addition, the mean values and standard deviations for the group delay time *tgr* as phase characteristics were also computed. Separation into Love wave and Rayleigh wave by coordinate transformation into the transverse and radial components from the NS and EW elements was difficult because of the complicated wave propagation in the 3D basin structure. In this study, the two horizontal components were synthesized and evaluated. First, the vectors comprising the two horizontal components were evaluated in all directions at intervals of 15°. Then, the maximum values of ${}_pS_V$ and mean values of *tgr* for each direction were used.

The difference in the magnitude and geometric and inelastic attenuation of each earthquake record was corrected based on Boore [8]. Earthquake records were normalized to a record corresponding to Mw 7.0 and hypocentral distance of 200 km based on the assumption that the Q_S value was 400 and the V_S value was 3.2 km/s. During the process, the seismic moment M_0 used was referenced from the values of the Earthquake Monthly Reports published by Japan Meteorological Agency. In cases where no values had been reported, the values of the F-net [7] were used. Further, in cases where the two values above were not available, values from Harvard University were used. The corner frequency f_c was calculated from the relation of f_c and M_0 as evaluated by Kawase and Matsuo [9] in their analysis of earthquakes in Japan.

Furthermore, to compare the characteristics of the body wave portion with the full records including surface wave, the body wave components were separated from the full records. For selection of the body wave components, the mean values of *tgr* (μ_{tgr}) and the standard deviations of *tgr* (σ_{tgr}) were used. The center of the each wave group for each period is indicated by μ_{tgr} while σ_{tgr} indicates the duration of each wave group for each period (Sawada et al. [10]). The high frequency body wave was dominant and μ_{tgr} was almost flat or independent of frequency. Therefore, the mean values of $\mu+\sigma_{tgr}$ were averaged from 1.0 Hz to 5.0 Hz as the end of body wave elements. Figure 2 shows an example of the selections. It was confirmed that the selected section of the body wave based on *tgr* was approximately compatible with visual judgments.

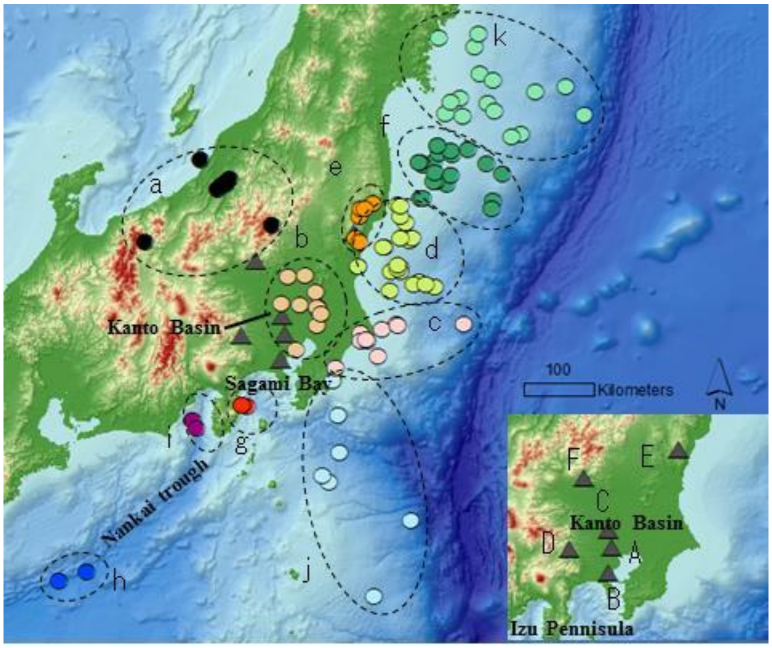

Fig. 1 – Location of the hypocenters, the earthquake groups and the recording stations

hypocenter earthquake group station

Table 1 – Outline of the recording station

	Code	Lat.	Lon.	Height (m)	Rock/Basin
A	TKY007	35.7107	139.6859	34.0	Basin
B	KNG002	35.4371	139.6340	2.0	Basin
C	SIT010	35.9065	139.6481	12.8	Basin
D	TKYH13	35.7017	139.1275	360	Rock
E	IBRH13	36.7955	140.5750	505	Rock
F	GNMH14	36.4931	139.3219	360	Rock

Table 2 – Outline of the earthquake groups

Group	M_{JMA}			Depth (km)			Number
a	5.1	–	6.8	4.6	–	16.8	8
b	5.1	–	5.9	43.7	–	78.8	11
c	5.0	–	6.6	11.2	–	50.7	11
d	5.0	–	6.5	31.8	–	57.3	21
e	5.2	–	6.4	6.6	–	16.7	6
f	5.1	–	7.0	13.4	–	51.2	22
g	5.0	–	5.8	4.0	–	7.1	3
h	7.1	–	7.4	37.6	–	43.5	2
i	6.2	–	6.5	23.0	–	23.3	2
j	5.0	–	6.6	56.1	–	90.7	7
k	5.1	–	7.3	7.0	–	86.3	16
							109

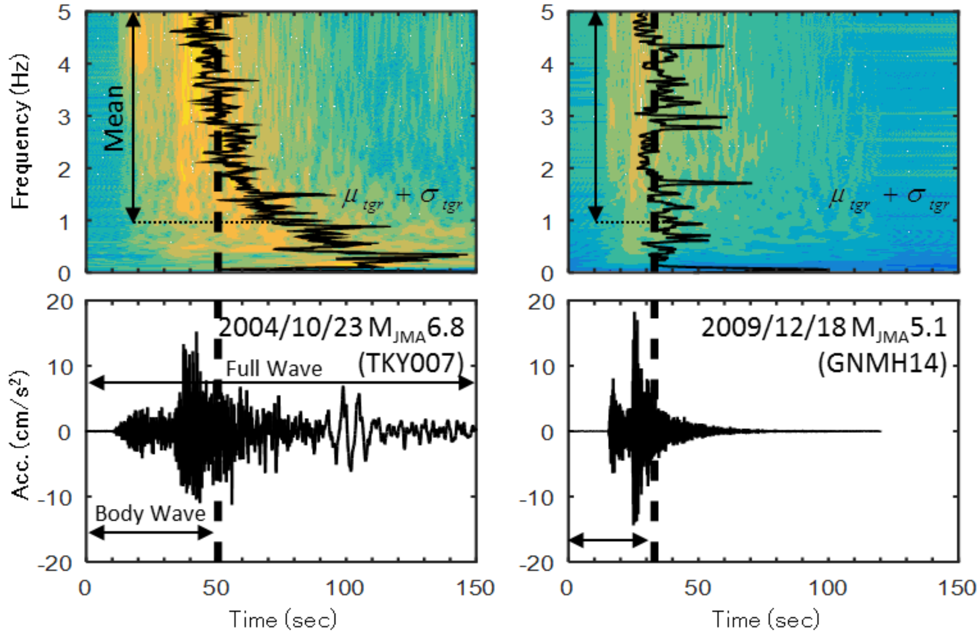

Fig.2 – Examples of body wave sections selected.

3. Amplification Spectrum Evaluation

The relationships of the pseudo velocity response spectra ${}_pS_V$ (cm/s) of the divided earthquake groups *a* – *k* were analyzed. Figure 3 shows the mean values for the ${}_pS_V$ computed from each group's record. The mean values of the ${}_pS_V$ varied from group to group. In some groups, the long-period components were strongly excited. The excitation in groups *a*, *g*, and *h* were strong, especially at the basin sites. In addition, the shapes of ${}_pS_V$ similarly changed. Furthermore, the group-to-group variations of ${}_pS_V$ at the basin sites (A, B, C) were larger than at the rock sites (D, E, F). The long-period components at the rock sites were also excited for groups *g* and *h*. The long-period components were inferred to be amplified by the accretionary wedge of the Nankai Trough and the thick sedimentary layers under the Sagami Bay rather than the sedimentary layers of the Kanto Basin.

The mean values and variation coefficients at each site were computed to evaluate the group-to-group variation of ${}_pS_V$. For the calculation, groups *g* and *h*, which were excluded from records, were not obtained at all sites. The ${}_pS_V$ values calculated from the full records, including the surface wave, were compared to values from the body wave parts in terms of variation width. Figure 4 shows the mean values and the variation coefficients of ${}_pS_V$ at each site. True values, rather than the logarithmic values, were used to calculate the mean values and variation coefficients.

Seismic waves were affected by the sedimentary layers of the Kanto Basin and the ${}_pS_V$ values at the basin sites were clearly larger than values at the rock sites. Furthermore, at the basin sites, the mean values of a full wave of ${}_pS_V$ were approximately twice as large as those of the body wave ${}_pS_V$ for the long-period. Therefore, the later part of records considerably contributed to the ${}_pS_V$ amplitudes. The variation coefficients of the full wave ${}_pS_V$ at the basin sites had peak values in the range 0.8–1.3 in 5 s–10 s periods, which had spectra with similar shapes. For the period range, the variation coefficients of body wave ${}_pS_V$ were about 0.5, which were clearly close to the values of the full wave ${}_pS_V$. Hence, the latter part of the records was dominant for the variation of long-period ground motion. On the other hand, judging from the minor difference in the variation coefficient values between full wave ${}_pS_V$ and body wave ${}_pS_V$, the latter part of the records did not contribute in that short 2-s period.

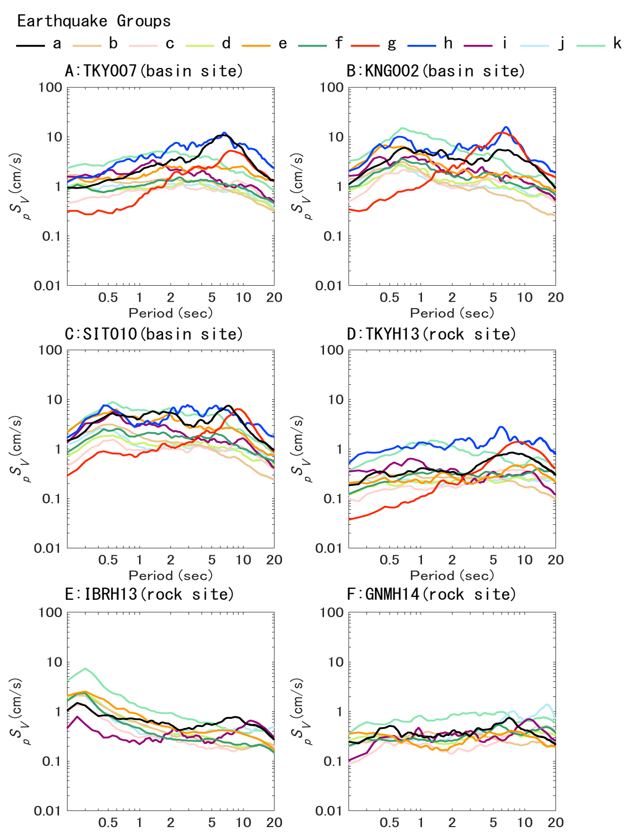

Fig.3 – Mean values for ${}_pS_V$ as computed from each group

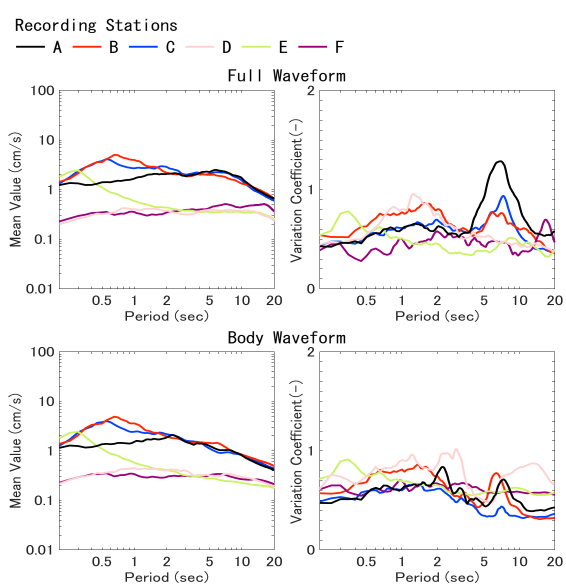

Fig.4 – Mean values and variation coefficients of ${}_pS_V$ at each site

4. Phase Spectrum Evaluation

4.1 Mean values for the group delay time μ_{tgr}

The relationships of the mean values for the group delay time μ_{tgr} (sec) to earthquake groups *a* - *k* were analyzed. The centers of the wave groups of each period are indicated by μ_{tgr}. Figure 5 shows the mean values of μ_{tgr} computed from each earthquake group. The shapes of the μ_{tgr} curves indicate dispersion for the case where surface waves are dominant. The value μ_{tgr} also varied depending on the groups. Additionally, for some groups μ_{tgr} was largely dispersed for the long-periods. However, the dispersion of the groups, except for *h*, changed in different manner relative to each other. For group *h*, long-period components were inferred to be strongly affected by the accretionary wedge of the Nankai trough before propagating in the Kanto Basin. Furthermore, the long-period components disperse at rock sites because of the excitation of the surface waves in the Kanto Basin or influences from external components of the basin such as group *h*.

Next, the mean values and variation coefficients of μ_{tgr} at each site were computed to evaluate the variations of μ_{tgr} quantitatively in the same manner as ${}_pS_V$. Figure 6 shows the mean values and the variation coefficients of μ_{tgr} at each site. The evaluation was carried out for the full wave and body wave components. The result from full wave shapes indicated that the sedimentary layers of the Kanto Basin dispersed the surface waves dispersing, and μ_{tgr} at the basin sites were larger than waves at the rock sites. Furthermore, the dispersion of the mean values of the body wave was slight. Therefore, the later part of the records contributed considerably to the μ_{tgr} dispersion. The variation coefficients of the full wave μ_{tgr} were approximately 0.1-0.2 and similar for each site. In the same period range, the variation coefficients of the body wave μ_{tgr} were approximately 0.05. Hence, the later part of the records was dominant for the variation of μ_{tgr} for the long-period.

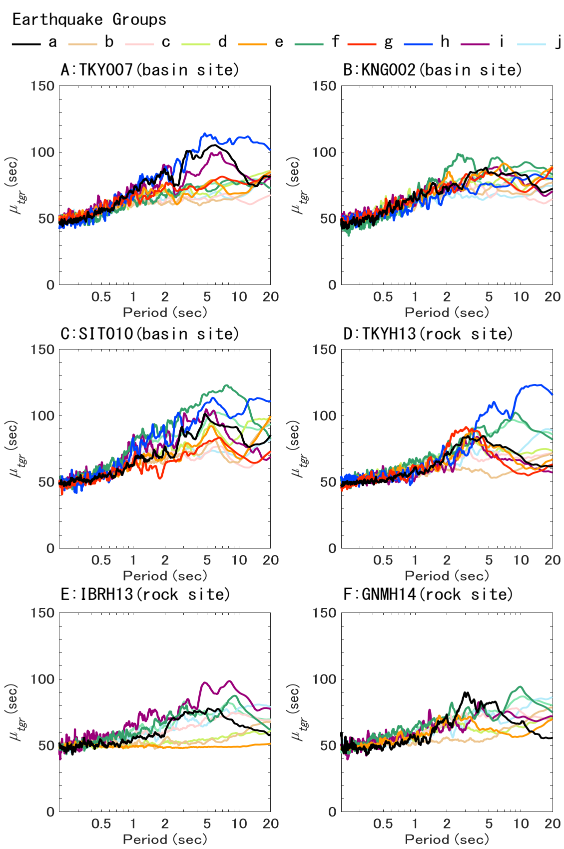

Fig.5 – Mean values for μ_{tgr} as computed from each group

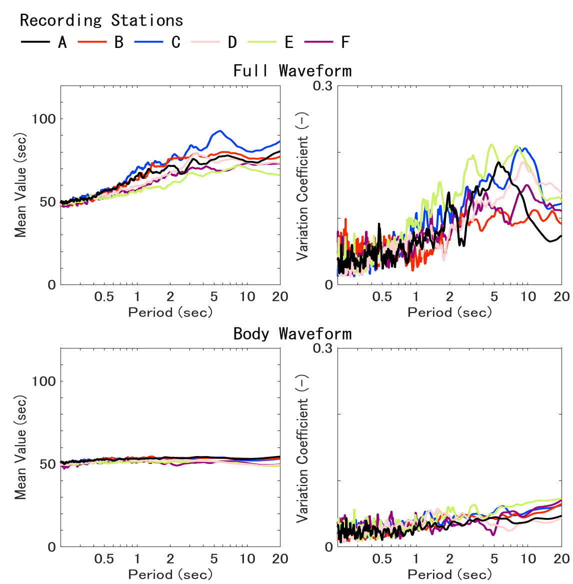

Fig.6 – Mean values and variation coefficients of μ_{tgr} at each site

4.2 Standard deviations of the group delay time σ_{tgr}

The relationships between the standard deviations of the group delay time σ_{tgr} (sec) and earthquake groups *a* - *k* were analyzed. The durations of the wave groups of each period were indicated by σ_{tgr}. Figure 7 shows the mean values for σ_{tgr} computed for each group. The mean values for σ_{tgr} also varied with the groups. Further, some long-period components dispersed similar to μ_{tgr}. However, the dispersion of the groups, except for *g*, changed in a different manner for each. For group *g*, the long-period components were inferred to be strongly affected by the thick sedimentary layers under the Sagami bay. Long-period components at rock sites also dispersed in a similar fashion to μ_{tgr}. Furthermore, at site E the mean values for σ_{tgr} of group *e* were smaller than for other groups. As the hypocenters of group *e* were almost directly under site E, the surface waves were slightly excited.

Next, the mean values and variation coefficients at each site were computed to quantitatively evaluate the variations of σ_{tgr} in the same manner as ${}_pS_V$. The evaluation was carried out for the full wave and body wave components. Figure 8 shows the mean values and the variation coefficients of σ_{tgr} at each site. The mean values at the basin sites were slightly different from the mean values at the rock sites, which was not the case for ${}_pS_V$ and σ_{tgr}. Furthermore, the mean values of the body wave were slightly dispersed. Hence, the latter part of the records contributed considerably to the dispersion of σ_{tgr}. The variation coefficients of the full wave σ_{tgr} dispersed slightly and had a similar value as the variation coefficients for the body wave σ_{tgr}. In addition, the variation coefficients for the body waves had similar values on each site. Therefore, the source characteristics may be dominant for the variation of σ_{tgr}.

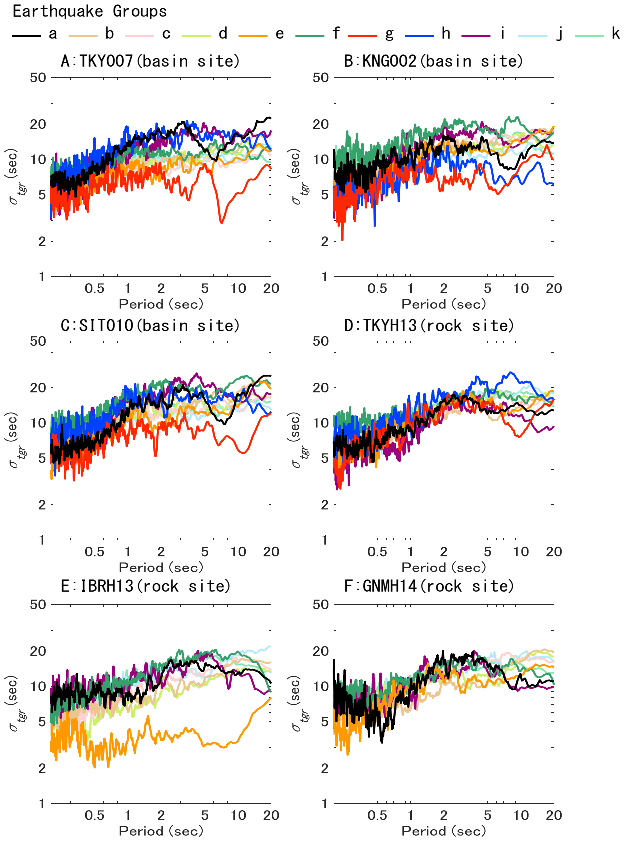

Fig.7 – Mean values for σ_{tgr} as computed from each group

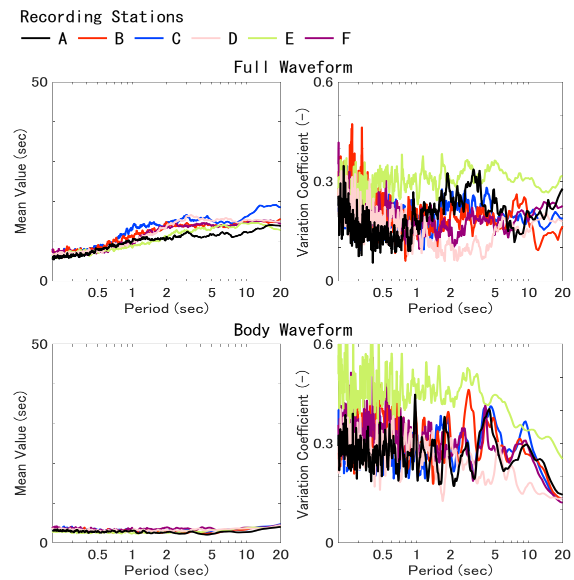

Fig.8 – Mean values and variation coefficients of σ_{tgr} at each site

5. Conclusion

To evaluate the variation in long-period ground motions, the relationships of the characteristics of ${}_pS_V$ and group delay time relative to the divided groups of the hypocenters were analyzed.

Consequently, it was found that the characteristics were different for each group. Further, these results virtually matched results from studies based on numerical simulations. The amplitudes (${}_pS_V$) at basin sites were larger than at the rock sites and the shapes of ${}_pS_V$ at each basin site similarly changed. Alternately, the shapes of the μ_{tgr} and σ_{tgr} curves each changed in a different manner.

The mean values and variation coefficients of ${}_pS_V$, μ_{tgr}, and σ_{tgr} at each site were then computed. The variation coefficients of full wave for ${}_pS_V$ and μ_{tgr} were larger than the coefficients for the body wave. Hence, the latter part of the records was dominant for the variation of long-period ground motion. Furthermore, the variation coefficients of ${}_pS_V$ at the basin sites were larger than the values at the rock sites. It was determined that the sedimentary basin was one of the factors for these variations. Alternately, the variation coefficients for the full wave σ_{tgr} exhibited similar values to the values for the body wave σ_{tgr}. This indicated that the source characteristics may be dominant in regards to the variation of the durations of the wave groups.

Dependence of the variation in long-period ground motions on the regions was confirmed. Therefore, the coefficients representing the variations were inferred to be separated from records based on spectral inversion. Detailed evaluations of the spectral inversion and extensive evaluations of the variation of the long-period ground motion by including more recording stations are considered necessary for future research in order to consider the variation in the structural design of long-period structures.

Acknowledgment

In this study, the records provided by K-NET and KiK-net [7] were used. We would like to thank all concerned.

6. References

[1] Hirai T, Fukuwa N (2013); Evaluation method of dynamic characteristics of sedimentary basin using 3-D finite difference method and reciprocity theorem, J. Struct. Constr. Eng., AIJ, 78, 694, 2083-2091, Dec, 2013.

[2] Terashima Y, Hirai T, Fukuwa N (2015); The effect of sedimentary basin structure on predominant period of seismic ground motion, J. Struct. Constr. Eng., AIJ, 80, 708, 219-229, Feb, 2015.

[3] Zama S (1993); Characteristics of long-period strong ground motion observed by JMA strong motion seismograph (Part 2: Tokyo), Report of Fire Research Institute of Japan, 76, 1-12, Sep, 1993.

[4] Uetake T (2010); Characteristics of long-period ground motion around Tokyo Bay area inferred from broadband earthquake observation, *The 13th Japan Earthquake Engineering Symposium, Japan*.

[5] Tsuno S, Yamanaka H, Midorikawa S, et al., (2012); Characteristics of long-period ground motions in the Tokyo metropolitan area and its vicinity, by recording data of the 2011 off the Pacific coast of Tohoku earthquake (Mw9.0) and the aftershocks, Journal of Japan Association for Earthquake Engineering, 12, 6, 102-116, 2012.

[6] Furumura T (2014); Risk of long-period ground motion due to the deep basement structure of the Kanto Basin, Journal of Geography (Chigaku Zasshi), **123**(4), 434-450, 2014.

[7] Okada Y, Kasahara K, Hori S, et al., (2004); Recent progress of seismic observation networks in Japan. -Hi-net, F-net, K-NET and KiK-net-, Earthquake Planets Space, 56, pp. xv-xxviii, 2004.

[8] Boore, D.M. (1983); Stochastic simulation of high-frequency ground motions based on seismological models of the radiated spectra, Bul. Seism. Soc. Amer., 73, 6, 1865-1894, 1983.

[9] Kawase H, Matsuo H (2004); Separation of source, path, and site effects based on the observed data by K-NET, KiK-net, and JMA strong motion network, Journal of Japan Association for Earthquake Engineering, 4, 1, 33-52, 2004.

[10] Sawada S, Morikawa H, Toki K, Yokoyama K (1998); Identification of path and local site effects on phase spectrum of seismic motion, *The 10th Japan Earthquake Engineering Symposium, Japan*.